Bioconjugate Chemistry

Communication

pubs.acs.org/bc

Third Generation Photo-Cross-Linked Small-Molecule Affinity Matrix: A Photoactivatable and Photocleavable System Enabling Quantitative Analysis of the Photo-Cross-Linked Small Molecules and Their Target Purification

Takahiro Suzuki,[†] Toshitaka Okamura,[†] Takenori Tomohiro,[‡] Yoshiharu Iwabuchi,[†] and Naoki Kanoh*,[†]

[†]Graduate School of Pharmaceutical Sciences, Tohoku University, 6-3 Aza-aoba, Aramaki, Aoba-ku, Sendai 980-8578, Japan

[‡]Graduate School of Medicine and Pharmaceutical Sciences, University of Toyama, 2630 Sugitani, Toyama 930-0194, Japan

Supporting Information

ABSTRACT: The third generation of photoactivatable beads designed to capture bioactive small molecules in a chemo- and site-nonselective manner upon irradiation at 365 nm of UV light and release them as coumarin conjugates after exposure to UV light of 302 nm is described. These photoactivatable and photocleavable beads enable quantification of the amount and distribution of immobilized small molecules prior to the pull-down experiments to identify target protein(s) for the immobilized small molecules. The newly developed system was then used to analyze the functional group compatibility of the photo-cross-linking technology as well as the preferable nature of small molecules to be immobilized. As a result, compounds having a hydroxyl group, carboxylic acid, or aromatic ring were shown to give multiple conjugates, indicating that these compounds are well compatible with the photoactivatable beads system.

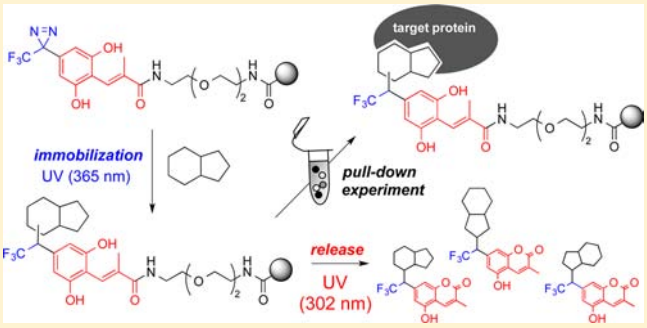

Proteins are one of the most important targets for bioactive small molecules. To date, many bioactive small molecules and drugs have been shown to interact with their protein targets to exert their biological activity. Therefore, identification (ID) of target proteins for bioactive small molecules has been one of the main topics in both academic and pharmaceutical research, and various target ID technologies have been developed as a result of this focus.[1,2] Small-molecule-immobilized affinity beads are a classical and highly valuable tool for target protein ID research, because affinity purification using these beads allows one-step purification of the target proteins from cell lysates.[3,4] Traditionally, prior to preparation of the small-molecule-immobilized beads, a structure−activity relationship (SAR) study is carried out to determine the site of affinity-beads attachment on each small molecule, because the selection of an appropriate site of attachment is important to discern correct target proteins for small molecules.[5−7] Although various useful methodologies have been developed for efficient SAR study and target protein ID,[8] the SAR study is still a major bottleneck in the target ID process. In addition to the difficulties associated with SAR study, recent studies have indicated that bioactive small molecules tend to interact with multiple targets, including on-targets and off-targets.[1,9] Therefore, obtaining all possible targets for a small molecule of interest is a very important issue.

To avoid the bottleneck associated with SAR study and maximize the possibility of ferreting out all possible protein targets, we have developed a rapid and widely applicable technology to immobilize small molecules in a chemo- and site-nonselective manner on an affinity matrix by using a photo-cross-linking reaction.[10] In this method, bead-immobilized trifluoromethyl aryl diazirine groups are used to capture small molecules of interest. Upon irradiation with 365 nm of UV light, aryl diazirines on the "photoactivatable" beads are activated and generate highly active carbene species, which in turn cross-link nearby small molecules that have been premixed with the beads. The small-molecule-immobilized beads thus prepared are ready for use in protein pull-down experiments (Figure 1A). The photogenerated carbene species are so reactive that the carbenes are expected to react with small molecules in a chemo- and site-nonselective manner. Indeed, we have shown that the photogenerated carbenes react with low-molecular-weight alcohols in a highly chemo-nonselective manner when the photolysis is carried out in the solid state.[11] By using this photo-cross-linking technology, we and others have immobilized various bioactive small molecules on photoactivatable beads to prepare small-molecule-immobilized beads, and direct interactions between the bioactive small molecules and their target proteins have been

Received: December 1, 2014
Revised: February 6, 2015
Published: February 10, 2015

DOI: 10.1021/bc500559e
Bioconjugate Chem. 2015, 26, 389−395

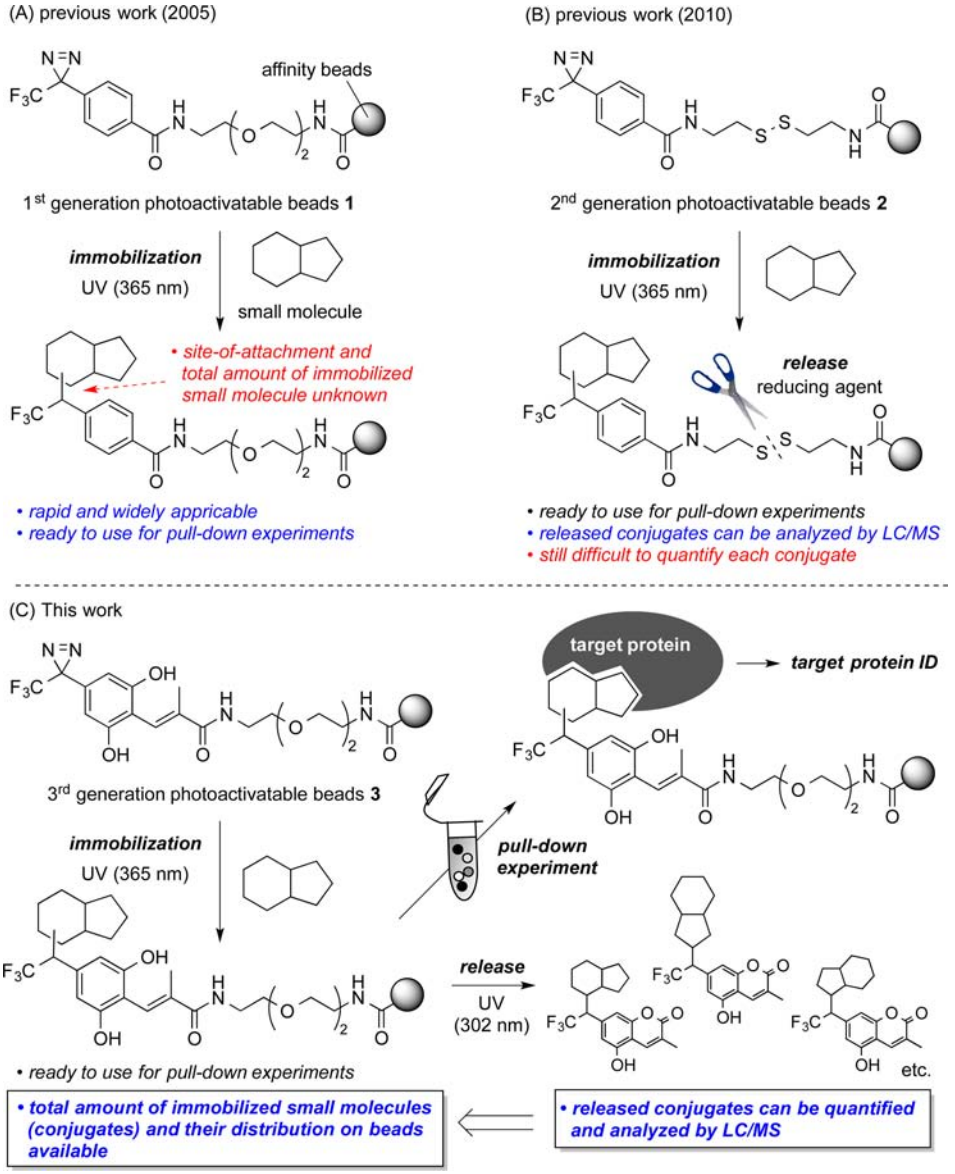

Figure 1. Photoativatable beads: (A) first generation, (B) second generation, and (C) third generation (this work).

successfully identified.[12−19] However, it has been pointed out that the photo-cross-linking technique cannot relay any information on the site of attachment, on the degree of bioactivity retained after immobilization, or on any design problems in the case of a failure to identify the target proteins.[20] To overcome these limitations, we developed second generation photoactivatable beads (beads **2**), in which a chemically cleavable disulfide bond was introduced between the bead and the diazirine group (Figure 1B).[21] Although the introduction of the cleavable site in beads **2** made it possible not only to verify the presence of the immobilized small molecule, but also to permit the efficient detection of proteins covalently bound to the immobilized small molecule, it was still difficult to quantify the immobilized small molecule on beads because the released small molecules themselves did not have any signature (e.g., characteristic UV absorption or fluorescence) that could be used for quantitative analysis.

Recently, Tomohiro et al. developed a unique protein-labeling strategy using a new diazirine-based photo-cross-linker containing an *O*-hydroxycinnamoyl unit.[22] They utilized two wavelength-dependent photoreactions for the protein labeling, i.e., photolysis of the diazirine group by 360 nm of UV light, and *E*-to-*Z* photoisomerization of the cinnamoyl group by irradiation at 315 nm to construct a coumarin fluorophore. We thought that the two wavelength photoreaction system could be utilized to develop a new photoactivatable bead. In this Communication, we report third generation photoactivatable beads (beads **3**), which immobilize small molecules through a first UV irradiation for protein pull-down experiments, and release the immobilized small molecule as coumarin conjugates after a second irradiation using a different wavelength of UV light (Figure 1C). The coumarin moiety in the conjugates allowed us for the first time to quantify the amounts of small molecules released (i.e., immobilized) by using LC/MS equipped with a photodiode array detector. This process was designed to determine the total amount of immobilized small molecules (i.e., photo-cross-linked conjugates) and their distribution on photoactivatable beads prior to the protein pull-down experiment. In addition, by using this photocleaving system, we analyzed the product distribution of the photo-cross-linked products from model small molecules

DOI: 10.1021/bc500559e
Bioconjugate Chem. 2015, 26, 389−395

Scheme 1. Preparation of Third Generation Photoactivatable Beads 3[a]

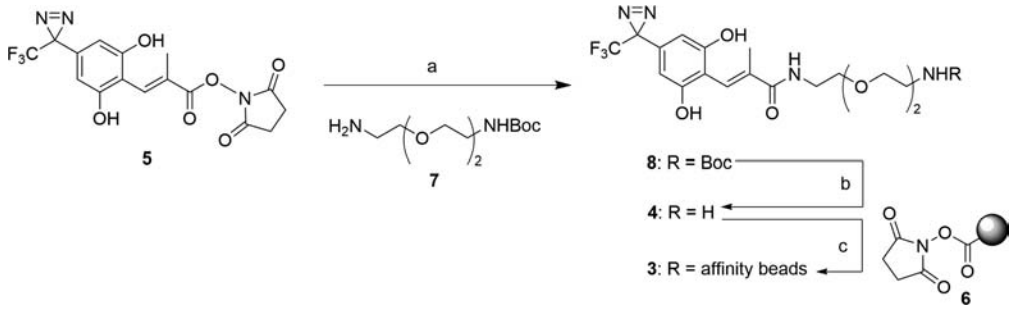

[a]Reagents and conditions: (a) **7**, MeCN, 25 °C, 0.5 h, 93%; (b) TFA-CH_2Cl_2 (1:9), 0 to 25 °C, 0.5 h, 99%; (c) NHS-activated Sepharose beads **6**, DMF, 25 °C, 1 h, then 1.0 M aq ethanolamine, 25 °C, 1 h. NHS: *N*-hydroxysuccinimide; DMF: *N*,*N*-dimethylformamide; Boc: *tert*-butoxycarbonyl; TFA: trifluoroacetic acid.

having a single functional group to access the functional group compatibility of the photo-cross-linking technology.

The beads **3** were prepared as follows: the known *N*-hydroxysuccinimidyl ester **5**[22] was coupled with mono-Boc protected amine **7**,[23] and deprotection of the Boc group of the resulting amide **8** gave amine **4** in good yield (Scheme 1). Introduction of **4** on Sepharose beads **6** followed by blocking of the resulting beads with 1.0 M aqueous ethanolamine gave the photoactivatable, photocleavable beads **3**.

First, we compared the affinity purification ability of beads **3** with that of beads **1**. We immobilized a bioactive cyclic peptide cyclosporin A (CsA)[24] onto beads **1** and **3** by using our reported procedure.[10] Specifically, a MeOH solution of CsA was mixed with the respective beads, and the mixture was concentrated and dried *in vacuo*. The CSA-premixed and dried beads were exposed to UV light (365 nm, 15 min, 4 J/cm^2), and then washed thoroughly in turn with MeOH, dimethyl sulfoxide (DMSO), and phosphate-buffered saline (PBS). Controls for both beads **1** and **3** were prepared by photolysis in the absence of CsA. To validate the ability of beads **3** to capture and purify the binding protein, beads **1** and **3** and their controls were incubated with Jurkat cell lysate, and the bead-bound proteins were separated by SDS-PAGE and visualized by Coomassie Brilliant Blue (CBB) staining (Figure 2). As a result, cyclophilin A (CypA), a cellular target of cyclosporin A,[24] was found to bind to both CsA-immobilized beads **1** and **3** to a similar extent (Figure 2, lanes 3 and 5) but not to either of the control beads (Figure 2, lanes 2 and 4). These experiments clearly showed that the third generation photoactivatable beads could be used in affinity purification experiments as well.

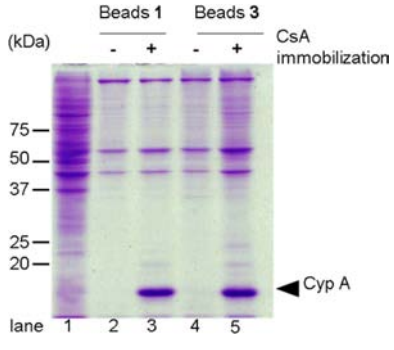

Figure 2. Detection of CsA-binding proteins in Jurkat cell lysate. Jurkat cell lysate was incubated with CsA-immobilized beads **1** and **3** (lanes 3 and 5, respectively) and their controls (lanes 2 and 4, respectively). The beads were then washed with lysis buffer containing 0.3% Triton X-100, resuspended in SDS sample buffer, and heated, and then the eluted proteins were separated by SDS-PAGE. The gel was visualized with CBB staining. Lane 1: Jurkat cell lysate (loading control).

Then, to check whether the photoinduced coumarin formation occurred efficiently in the solid phase, CsA-immobilized beads **3** were suspended in MeOH and irradiated at 302 nm. The UV absorption spectrum of the supernatant was typical of the absorption patterns of coumarin, having a maximum absorption at 298 nm, indicating that the coumarin formation took place as expected (see Supporting Information Figure S1).

For the successful quantitative analysis of the cleaved coumarin conjugates, it is necessary to check the difference in UV absorption intensity between the conjugates. Quantification by using the fluorescence intensity of the coumarin conjugates is also possible, but a UV detector is more common in typical HPLC systems. We therefore synthesized four coumarin derivatives **9**−**12** having different atoms (O, C, N, or S) at the benzylic position, analyzed them by LC, and recorded and plotted their integrated UV absorption intensity at 298 nm against the amount of each. As shown in Figure 3, the slope of the linear correlation between UV absorption and the amount of coumarin compound was essentially the same for all the compounds, indicating that this standard curve can be used to quantify the amounts of various coumarin conjugates.

Next, we analyzed the "on-bead" product distribution of the photo-cross-linked products. This type of analysis, which could not be performed by using first or second generation photoactivatable beads, was used not only to determine the exact product distribution on the beads, but also to optimize the immobilization conditions. Furthermore, the results of the analyses could be useful in creating guidelines for the use of the photoactivatable beads for various types of small molecules.

Toward this end, we selected 10 model compounds (cyclohexanol, phenol, hexanoic acid, *p*-methoxytoluene, 1,2-dimethoxybenzene, 2-adamantanol, dodecanethiol, 1-adamantane amine, methyl phenylalanate, and diethyl glutamate) that each have 1 of the 5 common functional groups found in bioactive small molecules (i.e., alcohol, amine, thiol, carboxylic acid, and aromatics).[25] These compounds were immobilized on the beads **3** by UV irradiation at 365 nm (15 min, 4 J/cm^2) at 25 °C. Coumarin formation from these compounds was negligible under these conditions (see Figure S2 in the Supporting Information). The immobilized molecules were cleaved in MeOH-d_4 as coumarin conjugates by UV irradiation at 302 nm (1 h, 20 J/cm^2) and 25 °C, and quantified by their integrated UV absorption

DOI: 10.1021/bc500559e
Bioconjugate Chem. 2015, 26, 389−395

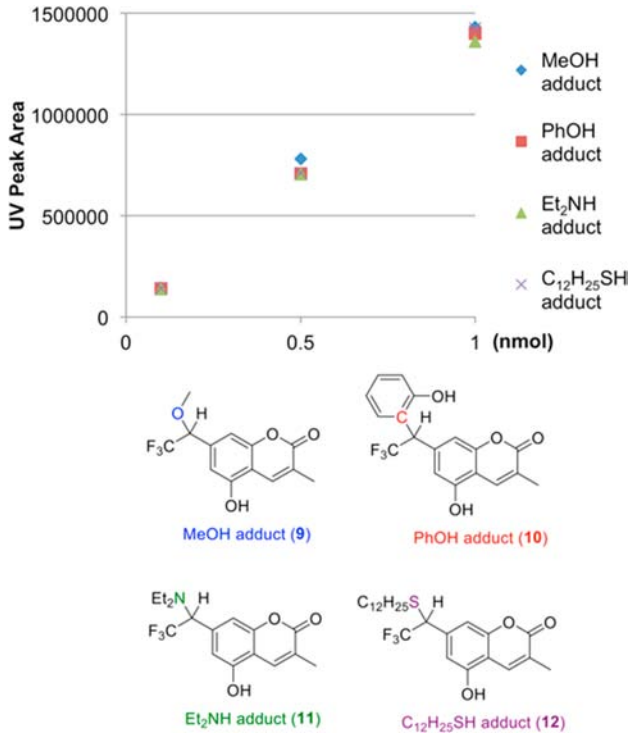

Figure 3. Relationships between the amount and the UV absorption intensity of coumarin compounds having different atoms at the benzylic position. Each of the compounds was analyzed by LC/MS and detected at 298 nm.

intensity at 298 nm. The use of MeOH-d_4 in the photoinduced cleavage reaction made it possible to discriminate the MeOH insertion product from unreacted diazirine and the isomerized diazo compound after the first photolysis (*vide infra*). After separation of the cleaved coumarin conjugates by using LC/MS, the molecular weights of the cleaved products were determined by the extracted ion chromatograms (XICs). The structures of major products from each small molecule were determined by comparison with the synthetic authentic samples (see Figure S3–S18 of the Supporting Information).

Figure 4 shows the chromatograms of photocleaved coumarins from cyclohexanol (CyOH)-immobilized beads **3**. By optimizing the LC conditions, the UV absorbance peaks at 298 nm were sufficiently resolved (Figure 4A), and they were classified by their molecular weights by the XICs (Figure 4B–F). Photocleaved coumarins derived from photo-cross-linked CyOH were observed at m/z 357 ($M+H^+$) (Figure 4B). The structure of the compound eluted at 37 min was determined to be that of the O–H insertion product **P1**. The compounds eluted at around 23 to 30 min were thought to be constitutional isomers and diastereoisomers of the possible C–H insertion products, although the structure of these compounds could not be fully determined because of the limited supply of materials. In addition to these desired CyOH-photo-cross-linked products, byproducts such as the formal H_2O adduct **P2** (Figure 4C), a formal reduced product **P3** (Figure 4D), two MeOH adducts **P4** and **P5** (Figure 4E), and a CD_3OD adduct **P6** (Figure 4F) were also observed. It should be noted that the intensity and position of peaks other than **P3** in Figure 4D varied depending on the small molecule used, suggesting that these peaks represented daughter ions of other ions. As described above, MeOH insertion products were derived from the reaction of photogenerated carbene with MeOH, which was used to mix affinity beads and CyOH, but remained in sepharose beads even after the extensive drying. The CD_3OD insertion product **P6** was clearly derived from unreacted diazirine and/or a diazo compound that was generated by the photoinduced isomerization of diazirine: i.e., the amount of **P6** was equal to the amount of **P7** (Scheme 2). The ratio of the amount of the MeOH-insertion product **P5** to that of the CD_3OD-insertion product **P6** could be calculated from the ratio of XIC peak intensity of the respective ions (Figure 4E,F).

The amounts of each photocleaved coumarin conjugate described above were quantified by using (1) the UV peak area intensity of coumarin derivatives and (2) the standard curve shown in Figure 3, as well as (3) the ratio of the XIC peak intensity of the MeOH-insertion product to that of the CD_3OD-insertion product. We performed the same type of analysis for the other 9 model compounds, and the results are summarized in Figure 5. A control experiment, in which diazirine photoactivation at 365 nm was performed in the absence of small molecules, was also carried out and the results are shown in Figure 5A. In the control experiment, the total amount of photocleaved coumarins **P2**–**P5** and **P7** was calculated to be 3.10 ± 0.22 μmol/mL of beads used, while the amount of diazirine groups introduced on beads **3** was estimated to be 4.64 ± 0.19 μmol/mL of beads.[26] This result showed that roughly one-third of the total number of diazirine groups on the beads was consumed for intercross-linking within the sepharose beads, leaving two-thirds available for the immobilization of small molecules.

In the case of the CyOH photo-cross-linking experiment, 38% of the available diazirine (i.e., ca. 25% of total diazirine) was utilized for the desired small molecule immobilization (Figure 5B). Half of this total amount of diazirine was used for O–H insertion, and the other half was used for C–H insertions at various positions of CyOH. Similarly, when the O–H bond and C–H bond coexist in a single molecule (Figure 5B–D and 5G), both the O–H and C–H insertion reactions proceed to give their products. Interestingly, reaction with phenol gave three products, i.e., phenyl ether **P8** along with *ortho*- and *para*-substituted phenols **P9** and **P10** in a 5.7:1:2 ratio (Figure 5C). These substituted phenols **P9** and **P10** are thought to be produced by a Friedel–Crafts-type reaction between an ion pair (phenoxide anion and carbenium cation) generated via a singlet carbene.[27] Aromatic compounds (Figure 5C,E,F) reacted with the photogenerated carbene at various positions in a different manner to give multiple products—e.g., aromatic C–H insertion (**P9** and **P10**), benzylic C–H insertion (**P12**), cyclopropanation (**P14**), and cyclopropanation followed by electrocyclic reaction (**P13**).[28] Generation of multiple conjugates is thought to be advantageous for exhaustive identification of target proteins for bioactive small molecules. This result may account at least in part for the good compatibility of aromatic compounds with our photo-cross-linking technology.[12−19]

On the other hand, it was revealed that compounds having an amine or thiol functionality tend to react at these polar functional groups in a highly selective manner (Figure 5H–K). Also, crystalline or solid compounds tend to give low yields of conjugates (Figure 5G and I–K), mainly because of the lack of diazirine-accessible surface area. Collectively, these findings indicate that the photo-cross-linking efficiency and chemo-site-selectivity are highly affected by the type of functional groups and the crystallinity of the compound.

DOI: 10.1021/bc500559e
Bioconjugate Chem. 2015, 26, 389–395

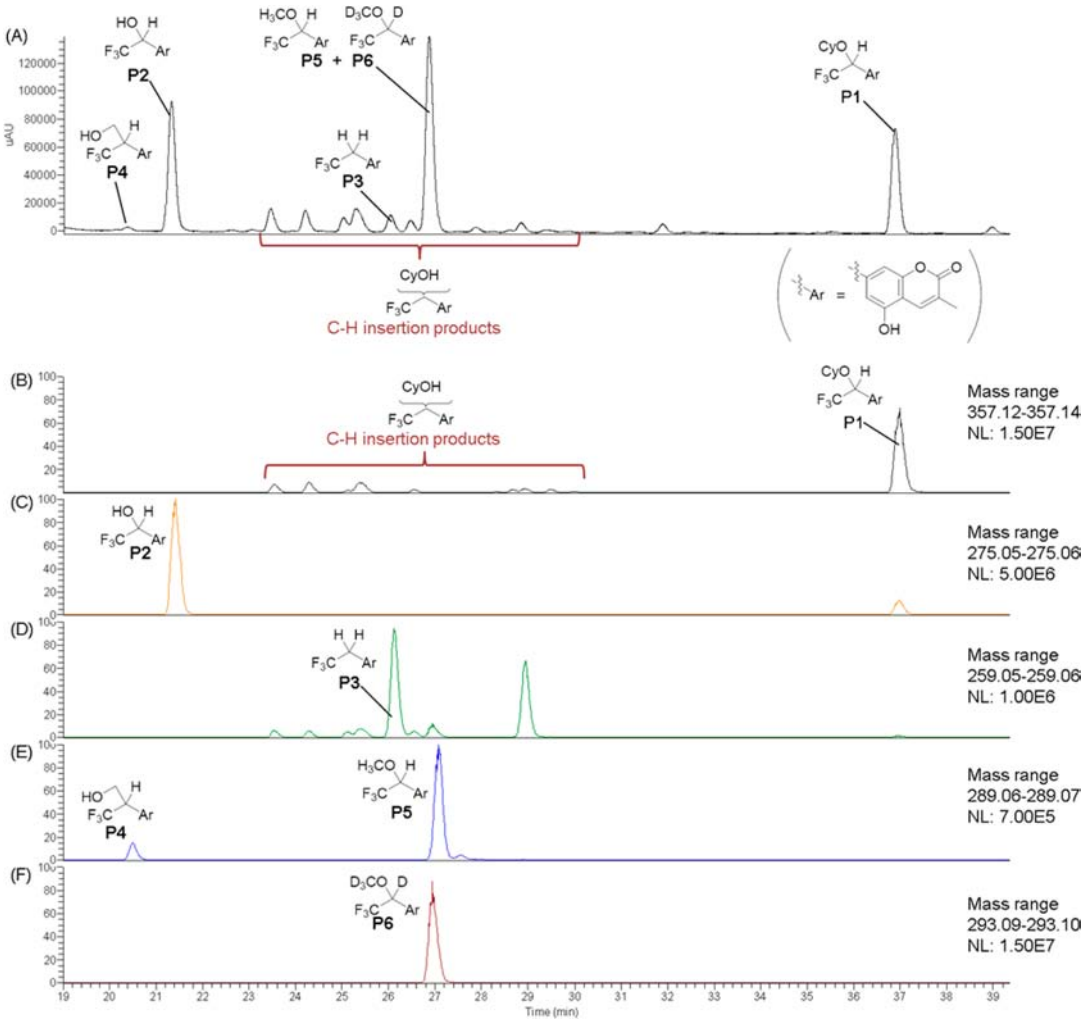

Figure 4. LC/MS analysis of photocleaved coumarin conjugates from CyOH-immobilized third generation beads. The UV chromatogram at 298 nm (A), and extracted-ion chromatograms (XICs) (B–F) are shown.

Scheme 2. Schematic Representation of the Generation of the MeOH Adduct P5 and CD_3OD Adduct P6

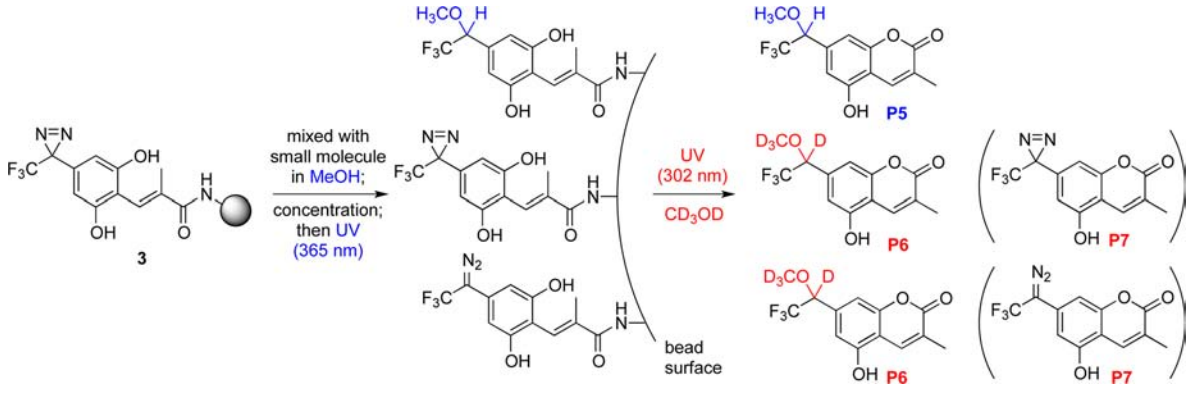

In conclusion, we have developed the third generation of our photoactivatable beads (beads **3**), and we demonstrated that these photoactivatable and photocleavable beads can be used not only for pull-down experiments, but also to quantify the amount and distribution of immobilized small molecules. By using this photoactivatable and photocleavable system, the photo-cross-linking reactions of model small molecules having a common functional group were analyzed, and compounds having a certain functional group, such as an alcohol, a carboxylic acid, or an aromatic ring, tended to give multiple different conjugates, as expected. On the other hand, some functional groups, such as amine and thiol, tended to react predominantly with the photogenerated carbene to produce an X–H insertion product (X = N or S). It was also shown that crystalline compounds are not well compatible with the photoactivatable bead system at the present time, although we have successfully immobilized crystalline CsA and biotin on a solid support by using this technology.[29] Although further

DOI: 10.1021/bc500559e
Bioconjugate Chem. 2015, 26, 389–395

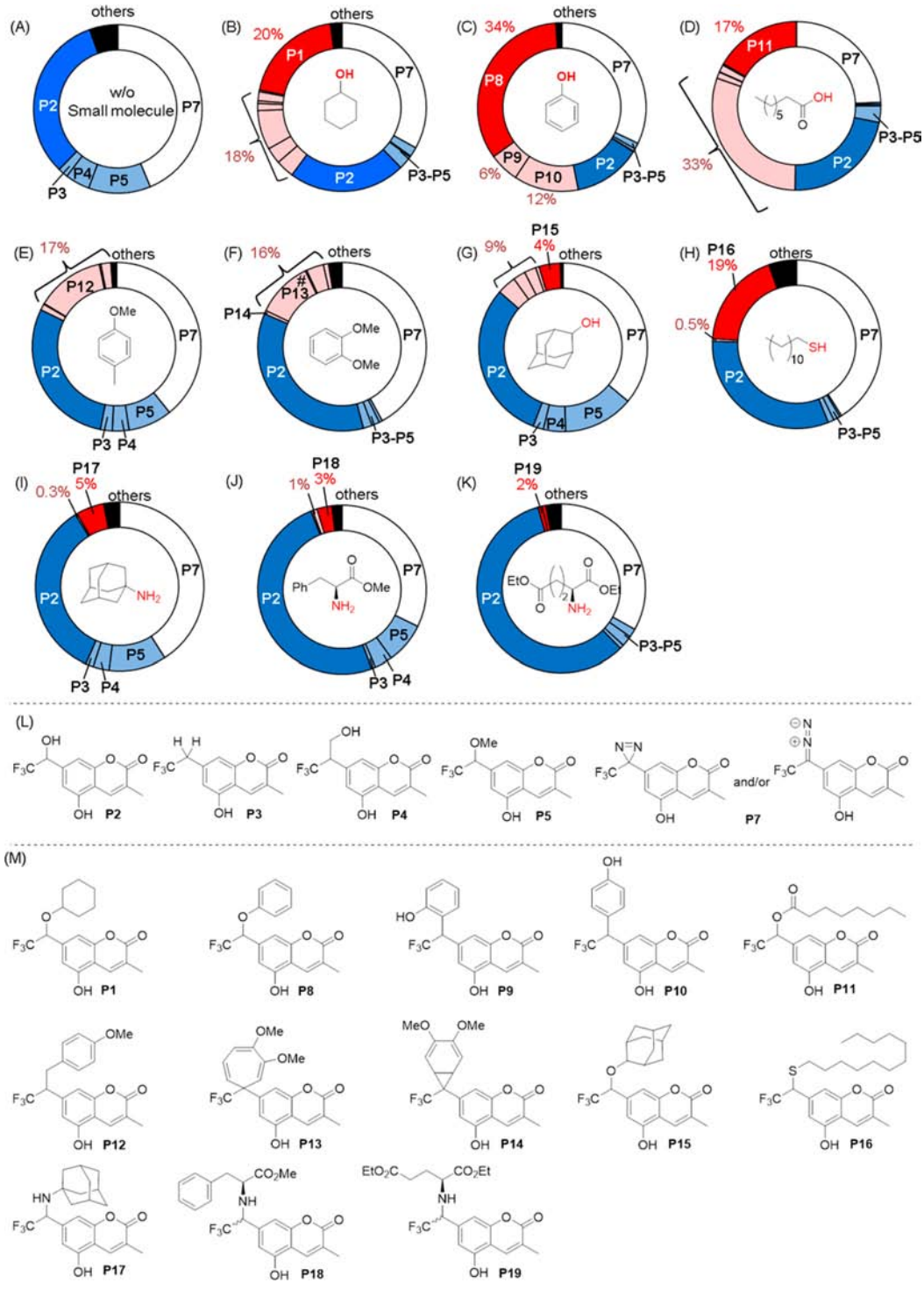

Figure 5. Quantitative analysis of photo-cross-linked product distribution. (A–K) Pie chart expression of the distribution of photocleaved coumarin conjugates from small molecule photo-cross-linked beads. The molecules shown in the center of each pie chart were used in the respective analysis. The regions of the pie chart shown in blue, light blue, red, and pink indicate the water insertion product **P2**, other side products **P3–P5**, X-H insertion products (X = O, S, and N), and other insertion/addition products, respectively. The section of the pie chart marked with a pound sign (#) contains conjugate **P13** and other unidentified conjugate(s) due to the peak overlap. (L) Structure of byproducts. (M) Structure of small molecule–coumarin conjugates.

reactivity analyses by using molecules having multifunctional groups are definitely needed, these third generation photoactivatable beads should allow us to identify and optimize reaction conditions suitable for the efficient photo-cross-linking of the small molecule of interest. Studies along these lines are now in progress.

■ ASSOCIATED CONTENT

Ⓢ Supporting Information

Details on the experimental protocols, characterization data, ^{1}H-, ^{13}C-, and ^{19}F-NMR spectra of synthesized compounds, UV chromatograms and XICs. This material is available free of charge via the Internet at http://pubs.acs.org.

DOI: 10.1021/bc500559e
Bioconjugate Chem. 2015, 26, 389–395

AUTHOR INFORMATION

Corresponding Author

*E-mail: nkanoh@m.tohoku.ac.jp. Phone and Fax: +81-22-795-6847.

Notes

The authors declare no competing financial interest.

ACKNOWLEDGMENTS

This work was partially supported by a Grant-in-Aid for Scientific Research on the Innovative Area "Chemical Biology of Natural Products" from The Ministry of Education, Culture, Sports, Science and Technology, Japan (No. 23102013 to N.K.).

REFERENCES

(1) Ueda, M. (2012) Chemical biology of natural products on the basis of identification of target proteins. *Chem. Lett. 41*, 658−666.

(2) Ziegler, S., Pries, V., Hedberg, C., and Waldmann, H. (2013) Target identification for small bioactive molecules: finding the needle in the haystack. *Angew. Chem., Int. Ed. 52*, 2744−2792.

(3) Leslie, B. J., and Hergenrother, P. J. (2008) Identification of the cellular targets of bioactive small organic molecules using affinity reagents. *Chem. Soc. Rev. 37*, 1347−1360.

(4) Sakamoto, S., Hatakeyama, M., Ito, T., and Handa, H. (2012) Tools and methodologies capable of isolating and identifying a target molecule for a bioactive compound. *Bioorg. Med. Chem. 20*, 1990−2001.

(5) Ki, S. W., Ishigami, K., Kitahara, T., Kasahara, K., Yoshida, M., and Horinouchi, S. (2000) Radicicol binds and inhibits mammalian ATP citrate lyase. *J. Biol. Chem. 275*, 39231−39236.

(6) Kim, E., and Park, J. M. (2003) Identification of novel target proteins of cyclic GMP signaling pathways using chemical proteomics. *J. Biochem. Mol. Biol. 36*, 299−304.

(7) Kanoh, N., Suzuki, T., Kawatani, M., Katou, Y., Osada, H., and Iwabuchi, Y. (2013) Dual structure-activity relationship of osteoclastogenesis inhibitor methyl gerfelin based on TEG scanning. *Bioconjugate Chem. 24*, 44−52.

(8) Robles, O., and Romo, D. (2014) Chemo- and site-selective derivatizations of natural products enabling biological studies. *Nat. Prod. Rep. 31*, 318−334.

(9) Hopkins, A. L. (2008) Network pharmacology: the next paradigm in drug discovery. *Nat. Chem. Biol. 4*, 682−690.

(10) Kanoh, N., Honda, K., Simizu, S., Muroi, M., and Osada, H. (2005) Photo-cross-linked small-molecule affinity matrix for facilitating forward and reverse chemical genetics. *Angew. Chem., Int. Ed. 44*, 3559−3562.

(11) Kanoh, N., Nakamura, T., Honda, K., Yamakoshi, H., Iwabuchi, Y., and Osada, H. (2008) Distribution of photo-cross-linked products from 3-aryl-3-trifluoromethyldiazirines and alcohols. *Tetrahedron 64*, 5692−5698.

(12) Kawatani, M., Okumura, H., Honda, K., Kanoh, N., Muroi, M., Dohmae, N., Takami, M., Kitagawa, M., Futamura, Y., Imoto, M., and Osada, H. (2008) The identification of an osteoclastogenesis inhibitor through the inhibition of glyoxalase I. *Proc. Natl. Acad. Sci. U.S.A. 105*, 11691−11696.

(13) Miyazaki, I., Simizu, S., Okumura, H., Takagi, S., and Osada, H. (2010) A small-molecule inhibitor shows that pirin regulates migration of melanoma cells. *Nat. Chem. Biol. 6*, 667−673.

(14) Ong, E. B. B., Watanabe, N., Saito, A., Futamura, Y., Abd El Galil, K. H., Koito, A., Najimudin, N., and Osada, H. (2011) Vipirinin, a Coumarin-based HIV-1 Vpr inhibitor, interacts with a hydrophobic region of VPR. *J. Biol. Chem. 286*, 14049−14056.

(15) Sasazawa, Y., Kanagaki, S., Tashiro, E., Nogawa, T., Muroi, M., Kondoh, Y., Osada, H., and Imoto, M. (2012) Xanthohumol impairs autophagosome maturation through direct inhibition of valosin-containing protein. *ACS Chem. Biol. 7*, 892−900.

(16) Hirohama, M., Kumar, A., Fukuda, I., Matsuoka, S., Igarashi, Y., Saitoh, H., Takagi, M., Shin-ya, K., Honda, K., Kondoh, Y., Saito, T., Nakao, Y., Osada, H., Zhang, K. Y. J., Yoshida, M., and Ito, A. (2013) Spectomycin B1 as a novel SUMOylation inhibitor that directly binds to SUMO E2. *ACS Chem. Biol. 8*, 2635−2642.

(17) Hayashi, K., Watanabe, B., Nakagawa, Y., Minami, S., and Morita, T. (2014) RPEL proteins are the molecular targets for CCG-1423, an inhibitor of Rho signaling. *PloS ONE 9*, e89016.

(18) Kawamura, T., Kondoh, Y., Muroi, M., Kawatani, M., and Osada, H. (2014) A small molecule that induces reactive oxygen species via cellular glutathione depletion. *Biochem. J. 463*, 53−63.

(19) Yao, R., Kondoh, Y., Natsume, Y., Yamanaka, H., Inoue, M., Toki, H., Takagi, R., Shimizu, T., Yamori, T., Osada, H., and Noda, T. (2014) A small compound targeting TACC3 revealed its different spatiotemporal contributions for spindle assembly in cancer cells. *Oncogene 33*, 4242−4252.

(20) Peddibhotla, S., Dang, Y. J., Liu, J. O., and Romo, D. (2007) Simultaneous arming and structure/activity studies of natural products employing O-H insertions: An expedient and versatile strategy for natural products-based chemical genetics. *J. Am. Chem. Soc. 129*, 12222−12231.

(21) Kanoh, N., Takayama, H., Honda, K., Moriya, T., Teruya, T., Simizu, S., Osada, H., and Iwabuchi, Y. (2010) Cleavable linker for photo-cross-linked small-molecule affinity matrix. *Bioconjugate Chem. 21*, 182−186.

(22) Tomohiro, T., Kato, K., Masuda, S., Kishi, H., and Hatanaka, Y. (2011) Photochemical construction of coumarin fluorophore on affinity-anchored protein. *Bioconjugate Chem. 22*, 315−318.

(23) Beer, P. D., Cadman, J., Lloris, J. M., Martinez-Manez, R., Soto, J., Pardo, T., and Marcos, M. D. (2000) Anion interaction with ferrocene-functionalised cyclic and open-chain polyaza and aza-oxa cycloalkanes. *J. Chem. Soc., Dalton Trans.*, 1805−1812.

(24) Handschumacher, R. E., Harding, M. W., Rice, J., and Drugge, R. J. (1984) Cyclophilin - a specific cytosolic binding-protein for cyclosporin-A. *Science 226*, 544−547.

(25) Henkel, T., Brunne, R. M., Muller, H., and Reichel, F. (1999) Statistical investigation into the structural complementarity of natural products and synthetic compounds. *Angew. Chem., Int. Ed. 38*, 643−647.

(26) Gaur, R. K., and Gupta, K. C. (1989) A spectrophotometric method for the estimation of amino-groups on polymer supports. *Anal. Biochem. 180*, 253−258.

(27) Raimer, B., and Lindel, T. (2013) Photoactivation of (p-methoxyphenyl)(trifluoromethyl)diazirine in the presence of phenolic reaction partners. *Chem.—Eur. J. 19*, 6551−6555.

(28) Ciganek, E. (1971) Cycloheptatriene-norcaradiene system 3. Dependence of ground-state enthalpy difference on substituents in 7-position. *J. Am. Chem. Soc. 93*, 2207−2215.

(29) Kanoh, N., Kumashiro, S., Simizu, S., Kondoh, Y., Hatakeyama, S., Tashiro, H., and Osada, H. (2003) Immobilization of natural products on glass slides by using a photoaffinity reaction and the detection of protein-small-molecule interactions. *Angew. Chem., Int. Ed. 42*, 5584−5587.

DOI: 10.1021/bc500559e
Bioconjugate Chem. 2015, 26, 389−395